

## CONCENTRATION OF SELECTED RADIONUCLIDES IN HIGH DUST DEPOSITION AREA: CONSIDERATION OF DEPLETED URANIUM

Abdulaziz Aba\*, Omar Al-Boloushi, Anfal Ismaeel

Kuwait Institute for Scientific Research, Kuwait City, Kuwait

**Abstract.** Fallen dust samples from ten Northern Arabian Gulf locations were analyzed for natural radionuclides and  $^{137}\text{Cs}$  using ultra-low background gamma spectrometry. A dust trap of 20 cm diameter collected the samples from ten sites in Kuwait, enabling the determination of radionuclide concentrations. Direct measurement of  $^{234}\text{Th}$  estimated  $^{238}\text{U}$ , while the  $^{235}\text{U}$  concentration was calculated using the sum peak of  $^{226}\text{Ra}$  and  $^{235}\text{U}$  of 186 keV gamma line. The calculation of the uranium activity ratio showed that the sample contained natural levels of uranium isotopes. The average concentration of various radionuclides demonstrated significant variation. The median concentrations of  $^7\text{Be}$ ,  $^{137}\text{Cs}$ ,  $^{210}\text{Pb}$ ,  $^{40}\text{K}$ ,  $^{224}\text{Ra}$ ,  $^{226}\text{Ra}$ ,  $^{228}\text{Ra}$  and  $^{234}\text{Th}$  were  $1113 \pm 148$ ,  $11.7 \pm 0.6$ ,  $434 \pm 27$ ,  $357 \pm 6$ ,  $23.4 \pm 1.7$ ,  $20.2 \pm 1.5$ ,  $12 \pm 2$  and  $44 \pm 1.8$  mBq  $\text{g}^{-1}$  respectively. The measured activity ratios of  $^{137}\text{Cs}/^{40}\text{K}$  and  $^7\text{Be}/^{210}\text{Pb}$  confirmed the effects of the regional dust sources.

**Keywords:** fallen dust, radium, depleted uranium, arid areas, Kuwait

### 1. INTRODUCTION

The issue of fallen dust becomes critical in countries most vulnerable to this natural climatic phenomenon, such as Middle Eastern countries, including Kuwait. It is widely recognized that dust can lead to adverse health effects, including respiratory and cardiovascular issues, as well as throat and eye irritation [1]. Additionally, areas with higher exposure to dust storms may experience negative economic impacts. Dust is usually loaded with various pollutants, such as rare metals, organic pollutants, and naturally or artificially occurring radioactive isotopes [2].

In addition, fine particulate matter with a diameter of fewer than 2.5 micrometers, known as PM<sub>2.5</sub>, can enter deep into lung tissues and spread throughout the body, causing various diseases, including allergies and respiratory diseases [3]. National regulatory authorities have adapted the world health organization reference levels [4] for air quality standards in this context. Accessing radiological information will support understanding the fallen dust characteristics and related hazards.

In this study, we investigated the radioactive airborne materials carried by dust, estimating the levels and concentrations of the deposited dust in Kuwait. Kuwait is a place that is frequently exposed to dust storms [5]. The focus was mainly on investigating the presence of the Depleted Uranium (DU), used during the Kuwait Liberation War 1991, where the amount of DU used was estimated at 300 tons [6]. During the Gulf War of DU were dropped in the aircraft rounds and tank-fired shells in Kuwait and southern Iraq over about 20,000 km<sup>2</sup> [7, 8]. The risks of inhaling DU have been

studied by many researchers, who have shown the extent of the danger of exposure and its long-term effects [9, 10, 11]. Regarding DU in Kuwait, the report issued by the International Atomic Energy Agency indicated that there was no radiation harm to the population in the country [12]. However, as is known, public reactions to such issues remain present from time to time. In order to assess the levels of hazardous, radioactive materials generally and work with regulatory authorities to mitigate their effects, it is necessary for the Kuwait Institute for Scientific Research (KISR) to provide accurate scientific information based on monitoring and experimentation. This monitoring involves a continuous radiation-monitoring program for the terrestrial, marine, and atmospheric environments within the country.

In this study, a non-destructive gamma spectrometry technique was employed to evaluate the concentration of specific radionuclides in fallen dust samples collected over a two-year period. The goal is to investigate the application of selected radionuclide ratios to understand both local and long-range dust transport, as well as to verify the presence of depleted uranium (DU).

### 2. METHODOLOGY

#### 2.1. Sampling and sample preparation

A PVC bucket with a single-piece construction, measuring 0.2 meters in diameter and 0.4 meters in depth, was employed to collect dust samples from ten locations in Kuwait (Figure 1). The bucket was half-filled with glass marble to prevent deposited dust in the bottom of the pan from being blown away. The dust

\* [aaba@kISR.edu.kw](mailto:aaba@kISR.edu.kw)

collectors were installed 3 m above ground and were far from being affected by the infrastructure. A composite sample was collected from 4 dust traps deployed in each location for almost a month to accumulate the adequate sample mass required for radioactivity analysis. The total net dry weight ranged from about 0.5 g to 15 g. The collected dust mass was bottled in a small vial (1 cm diameter and 3 cm length) filled with wax using a glue gun and stored for about three weeks. This step is necessary to attain the secular equilibrium between the  $^{222}\text{Rn}$  and its progenies  $^{214}\text{Pb}$  and  $^{214}\text{Bi}$  to determine the  $^{226}\text{Ra}$  content. The prepared samples were counted for more than 200,000 seconds to get a reasonable statistical peak area calculation (less than 10% area error) of the radionuclides of interest.

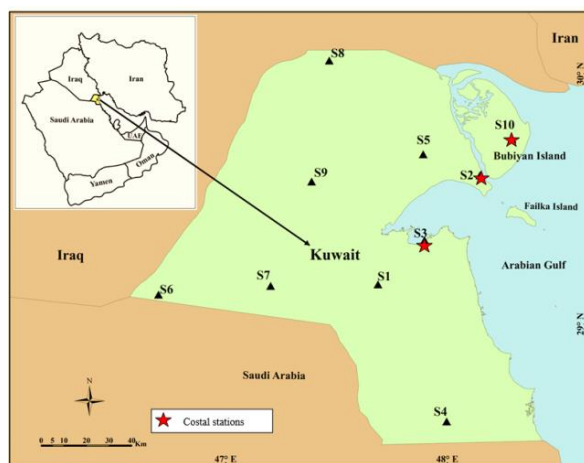


Figure 1. The location of the coastal and interior fallen dust samples

## 2.2. Gamma spectrometry measurements and analysis

An Ultra-Low Background (ULB) gamma spectrometry system, featuring a Canberra Broad Energy Germanium (BEGe) detector, was employed for measuring gamma emissions within the 5–3,000 keV range. The system boasts excellent low energy resolution, as evidenced by a Full Width at Half Maximum (FWHM) of 750 eV at 122 keV. This capability allows for the effective resolution of low energy peaks, including those of  $^{210}\text{Pb}$  and  $^{234}\text{Th}$ , with good statistical accuracy. The crucial feature of this spectrometry system lies in its well-designed shielding, which allows for the identification of both natural and artificial radionuclides, including low-energy gamma emitters, at remarkably low detectable activity levels. For instance, the system can achieve detection limits as low as 0.064 Bq for  $^7\text{Be}$ , 0.024 Bq for  $^{40}\text{K}$ , 0.004 Bq for  $^{137}\text{Cs}$ , and 0.043 Bq for  $^{210}\text{Pb}$ , across a sample mass ranging from 1 to 5 grams. The detector efficiency was calibrated using an in-house calibration source prepared by spiking dust samples with traceable gamma mixed standard solutions (QCYB-41 and QCYB-40) prepared by KDD Germany. The calibration source covers the energy range from 30 keV to 3 MeV. However, the efficiency correction due to different sample masses and cascade summing was performed by the Canberra-Genie 2000 analysis software. The radioactivity of  $^{137}\text{Cs}$  (661.6 keV),  $^{40}\text{K}$  (1460.8 keV),  $^{210}\text{Pb}$  (46.5 keV),  $^7\text{Be}$  (477.3 keV),  $^{224}\text{Ra}$  (238.6 and 583.6 keV),  $^{226}\text{Ra}$  (186.5 keV),  $^{228}\text{Ra}$  (338.2 and 911.2 keV), and  $^{234}\text{Th}$  (63.4 keV) determination was based on highly

intense gamma lines. However, the necessary correction for relatively short-lived radionuclide  $^7\text{Be}$  ( $t_{1/2} = 53.2$  d) during the sample collection period (i.e., 30 days) has been implemented.

## 2.3. Uranium isotopic ratio calculation

A gamma spectrometric measurement of the first uranium progeny ( $^{234}\text{Th}$ ) was used to calculate the activity contents of  $^{238}\text{U}$ , assuming a secular equilibrium state condition. The  $^{235}\text{U}$  concentration was calculated using the highest intense gamma line, 185.7 keV (0.57), and taking into consideration the interferences with the  $^{226}\text{Ra}$  gamma line (186.2 keV) of a low gamma yield (0.036). In the gamma spectrum, there is a comprehensive breakdown observed at the 186 keV gamma line, which includes the gamma counts of  $^{226}\text{Ra}$  and  $^{235}\text{U}$  in relation to their individual gamma yields (as shown in Figure 1). In this context, the determination of the 186 keV peak can be computed utilizing the subsequent methodology [13]:

The disintegration rate (DR) can be represented by the equation

$$\text{DR} = A \cdot \text{BR} \quad (1)$$

where A denotes the activity concentration and BR represents the gamma intensity.

According to Figure 1, the equation describing the total disintegration counts can be expressed as follows:

$$\text{DR}(^{226}\text{Ra})_{\text{tot}} = \text{DR}(^{235}\text{U}) + \text{DR}(^{226}\text{Ra}) \quad (2)$$

By utilizing equation (1), the total disintegration counts of  $^{226}\text{Ra}$  can be defined as:

$$\frac{\text{DR}(^{226}\text{Ra})_{\text{tot}}}{\text{BR}(^{226}\text{Ra})} = \frac{A(^{235}\text{U}) \cdot \text{BR}(^{235}\text{U}) + A(^{226}\text{Ra}) \cdot \text{BR}(^{226}\text{Ra})}{\text{BR}(^{226}\text{Ra})} \quad (3)$$

However,

$$\text{DR} = \text{CR}/(\text{m EFF}) \quad (4)$$

where CR symbolizes the count rate, m denotes the sample mass, and EFF represents the detector efficiency. Consequently, equation (3) transforms into:

$$\frac{\text{CR}(^{226}\text{Ra})_{\text{tot}}/(\text{m EFF})}{\text{BR}(^{226}\text{Ra})} = \frac{A(^{235}\text{U}) \cdot \text{BR}(^{235}\text{U}) + A(^{226}\text{Ra}) \cdot \text{BR}(^{226}\text{Ra})}{\text{BR}(^{226}\text{Ra})} \quad (5)$$

Thus, the activity concentration of  $^{235}\text{U}$  can be calculated based on the  $\text{CR}(^{226}\text{Ra})_{\text{tot}}$  gamma line and the assumption that  $^{226}\text{Ra}$  is in equilibrium with the activity concentration of  $^{214}\text{Pb}$  and  $^{214}\text{Bi}$ . This can be expressed by the following formula:

$$A(^{235}\text{U}) = \left\{ \left[ \frac{\text{CR}(^{226}\text{Ra})_{\text{tot}}}{\text{m} \cdot \text{EFF}} \right] - \left[ \frac{A(^{226}\text{Ra}) \cdot \text{BR}(^{226}\text{Ra})}{\text{BR}(^{235}\text{U})} \right] \right\} / \text{BR}(^{235}\text{U}) \quad (6)$$

The activity concentration ratio of  $^{235}\text{U}/^{238}\text{U}$  can be calculated and then compared with the corresponding ratios of natural uranium (0.0457) and depleted uranium (0.013) [9].

## 2.4. Quality assurance

Quality control procedure using an in-house control sample [14] was used to monitor the performance of the ULB gamma spectrometry system. The control sample contains a known amount of uranium ore, where gamma lines of  $^{210}\text{Pb}$ ,  $^{214}\text{Pb}$ , and  $^{214}\text{Bi}$  were used as control parameters in the Shewhart quality control chart. In addition, background variations and

environmental changes conditions within the laboratory were also monitored and controlled.

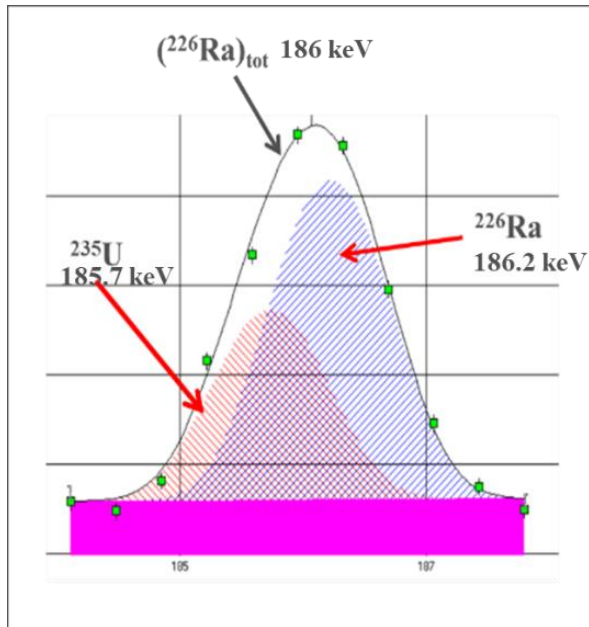


Figure 1. The total peak area of  $(^{226}\text{Ra})_{\text{tot}}$ ,  $^{235}\text{U}$  and  $^{226}\text{Ra}$  area peaks

### 3. RESULTS AND DISCUSSION

#### 3.1. Concentration of radionuclides associated with fallen dust

The explanatory data analysis of  $^{137}\text{Cs}$ ,  $^{210}\text{Pb}$ ,  $^7\text{Be}$ ,  $^{40}\text{K}$ ,  $^{224}\text{Ra}$ ,  $^{226}\text{Ra}$ ,  $^{228}\text{Ra}$ , and  $^{234}\text{Th}$  radionuclides concentration in the dust samples were presented in Box Plot form (Fig. 2).

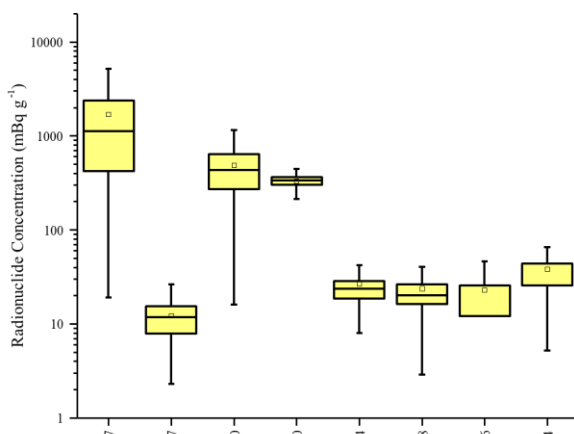


Figure 2. The explanatory of the  $^{137}\text{Cs}$ ,  $^{210}\text{Pb}$ ,  $^7\text{Be}$ ,  $^{40}\text{K}$ ,  $^{224}\text{Ra}$ ,  $^{226}\text{Ra}$ ,  $^{228}\text{Ra}$ , and  $^{234}\text{Th}$  radionuclides concentration in fallen dust samples collected between 2009-2011 in Kuwait

The results revealed a wide range of measurements for the concentration of radionuclides. This reflects the different parameters affecting dust deposition (e.g., precipitation rate, dust, sand storm occurrences, wind speed and direction, land use, etc.). The correlation coefficient between the mean levels of the fallout origin radionuclides ( $^7\text{Be}$ ,  $^{137}\text{Cs}$ ,  $^{210}\text{Pb}$ ) showed a significant statistical relationship. The order of significance for this

correlation was determined to be  $^7\text{Be}/^{210}\text{Pb} > ^{137}\text{Cs}/^{210}\text{Pb} > ^7\text{Be}/^{137}\text{Cs}$ , as shown in Table 1. This is likely reflecting the origin and transport of radionuclides associated with dust, including the effect of resuspension process. It was assumed that the highest correlation of ( $^7\text{Be}/^{210}\text{Pb}$ ) is most likely related to the resuspension associated with the local dust events [15].

Table 1. The correlation coefficient of  $^{210}\text{Pb}$ ,  $^{137}\text{Cs}$  and  $^7\text{Be}$  in the fallen dust

Parameters	Correlation Coefficient
$^7\text{Be}/^{210}\text{Pb}$	0.93
$^{137}\text{Cs}/^{210}\text{Pb}$	0.64
$^7\text{Be}/^{137}\text{Cs}$	0.58

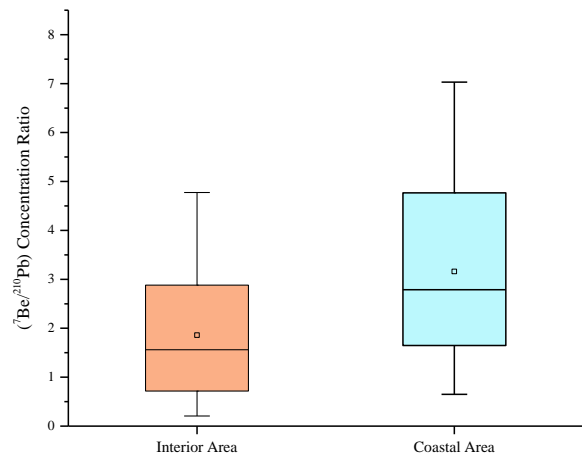


Figure 3-a. The concentration ratios of  $^7\text{Be}$  and  $^{210}\text{Pb}$  data set in fallen dust collected between 2009-2011 in Kuwait

Figure 3-a shows the variations in ratio between in the interior and the coastal region samples, with 69 samples from coastal and 161 from interior area. The mean ratio in the interior area is significantly lower ( $1.84 \pm 0.3$ ) than that of the coastal region ( $3.14 \pm 0.4$ ); a lower ratio means that the contribution of local resuspension dust of the interior is higher than that of the coastal area. This assumption can be valid if we take into account the short half-life of  $^7\text{Be}$  (53 d), that when the particle labelled  $^7\text{Be}$  travels longer distances, it will take longer time to reach the deposition area, which leads to  $^7\text{Be}$  decay and thus measuring less radioactivity content. In other words, these ratios' variation reflects the deposition mechanism difference. Additionally, the impact of local resuspension dust was examined through the radionuclide concentration ratio of the fallout origin  $^{137}\text{Cs}$  and  $^{40}\text{K}$  from the crustal origin (see Figure 3-b). In the interior area, the mean ratio is 1.77 smaller than that in the coastal region, indicating the influence of local crustal dust with higher  $^{40}\text{K}$  concentrations compared to the coastal counterpart.

On the other hand, the low correlation of the  $^7\text{Be}/^{137}\text{Cs}$  ratio (0.58) could be related to the long-range transport of  $^{137}\text{Cs}$  and  $^7\text{Be}$  loaded dust, where the half-lives play a significant role in decreasing the  $^7\text{Be}$  activity concentration.

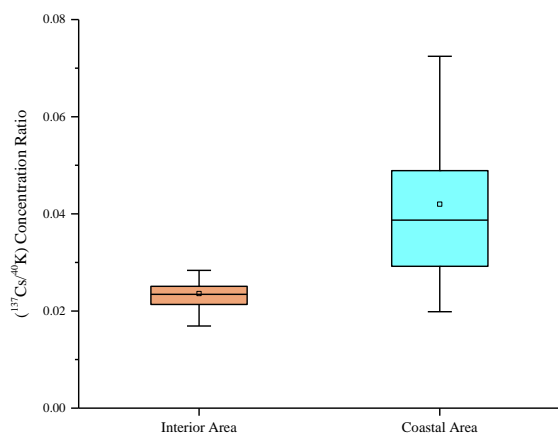


Figure 3-b. The concentration ratios of <sup>137</sup>Cs and <sup>40</sup>K in fallen dust samples collected in Kuwait

### 3.2. Calculation of <sup>235</sup>U/<sup>238</sup>U concentration ratio in dust samples

The calculated activity concentration of <sup>235</sup>U and <sup>238</sup>U through gamma measurements showed that the <sup>235</sup>U/<sup>238</sup>U activity ratio varied from 0.044 to 0.072 with an average value of 0.058 ± 0.014 mBq g<sup>-1</sup> (Table 2). This ratio is close to the <sup>235</sup>U/<sup>238</sup>U natural activity ratio found in the soil (0.0457) [16] and far beyond that found in depleted DU (0.013) [9]. According to Table 2, <sup>235</sup>U/<sup>238</sup>U calculated ratios were within the range of the natural activity ratio regardless of the sample location. The obtained results in this study agree with findings of the international group of experts on the radiological conditions in Kuwait in 2003 [12]. During the IAEA expert mission, many environmental samples, including dust, water, vegetation, and soil, were collected and analyzed using gamma, alpha spectrometry, and ICP-Ms to determine <sup>234</sup>U, <sup>235</sup>U, and <sup>238</sup>U mass and activity ratios. Although some DU was present in surface soil samples of the area bombarded with DU, the estimated annual radiation doses that could arise from exposure to DU residues would be very low and of little radiological concern [12].

Table 2. The calculation of <sup>235</sup> and <sup>238</sup>U ratios in fallen dust samples collected between 2009-2011 in Kuwait

Station/location	<sup>226</sup> Ra(a)	<sup>234</sup> Th(b)	<sup>235</sup> Ucal(c)	<sup>235</sup> U/ <sup>238</sup> U
	mBq g <sup>-1</sup>			
S-1 (29.704882, 48.238845)	14.1	44.0	2.29	0.052
S-2 (29.593734, 48.148385)	16.7	44.0	2.43	0.055
S-3 (29.365785, 47.742351)	14.8	42.7	2.22	0.052
S-4 (28.604661, 47.950101)	15.1	44.0	2.43	0.055
S-5 (29.727937, 47.915486)	14.6	43.3	2.40	0.056
S-6 (29.125670, 46.662896)	16.7	41.7	2.13	0.051
S-7 (29.166689, 47.166488)	28.6	24.6	1.63	0.066
S-8 (30.077159, 47.639021)	16.9	37.2	2.39	0.064
S-9 (29.587667, 47.551168)	16.7	44.0	2.82	0.064
S-10 (29.677499, 48.278214)	13.3	44.0	2.63	0.060

- a) Calculated based on <sup>214</sup>Pb and <sup>214</sup>Bi
- b) Assumed to be in equilibrium with <sup>238</sup>U
- c) Calculated from formula (3)

## 5. CONCLUSION

The concentration of radionuclides in dust fall out of two years of collected samples in Kuwait was determined using ULB. The radionuclides' concentrations were significantly varied due to

environmental parameters affecting dust deposition (resuspension and metrological conditions). The concentration ratios of the fallout origin <sup>210</sup>Pb, <sup>7</sup>Be, <sup>137</sup>Cs, and the crustal <sup>40</sup>K indicated the local and long-range dust transport contribution. The calculated ratios of <sup>235</sup>U/<sup>238</sup>U indicated that the fallen dust samples were free of DU. Using ULB gamma spectrometry equipped with BEGe can provide an accurate determination of low energies gamma lines (<sup>234</sup>Th). More accurate and precise results can be achieved using a radiochemical separation procedure.

**Acknowledgements:** The authors would like to thank Dr. Ali-Aldousari for his valuable comments. Also, thanks to the staff of KISR's Radioactivity Measurements Laboratory staff.

## REFERENCES

- A. Al-Hemoud et al., "Health impact assessment associated with exposure to PM10 and dust storms in Kuwait," *Atmosphere*, vol. 9, no. 1, 6, Jan. 2018. DOI: 10.3390/atmos9010006
- A. Aba, A. Ismaeel, A. Al-Boloushi, H. Al-Shammari, O. Al-Boloushi, "Deposited Rates of Radionuclides," in *Atlas of Fallen Dust in Kuwait*, A. Al-Dousari, Eds., 1<sup>st</sup> ed., Cham, Switzerland: Springer Cham, 2021, ch. 6, pp. 140 – 176. DOI: 10.1007/978-3-030-66977-5\_6
- A. Al-Hemoud et al., "Sand and dust storm trajectories from Iraq Mesopotamian flood plain to Kuwait," *Sci. Total Environ.*, vol. 710, 136291, Mar. 2020. DOI: 10.1016/j.scitotenv.2019.136291 PMID: 31911252
- What are the WHO Air quality guidelines? Improving health by reducing air pollution*, WHO, Geneva, Switzerland, 2021.
- A. Al-Dousari, N. Al-Dousari, "Deposited Dust," in *Atlas of Fallen Dust in Kuwait*, A. Al-Dousari, Eds., 1<sup>st</sup> ed., Cham, Switzerland: Springer Cham, 2021, ch. 2, pp. 47 – 56. DOI: 10.1007/978-3-030-66977-5\_2
- H. Bem, F. Bou-Rabee, "Environmental and health consequences of depleted uranium use in the 1991 Gulf War," *Environ. Int.*, vol. 30, no. 1, pp. 123 – 134, Mar. 2004. DOI: 10.1016/S0160-4120(03)00151-X PMID: 14664872
- E. G. Daxon et al., *Health and Environmental Consequences of Depleted Uranium Use in the U.S. Army: Technical Report*, Rep. AEPI-0038, AEPI, Atlanta (GA), USA, 1995. Retrieved from: [https://www.academia.edu/25782366/Health\\_and\\_Environmental\\_Consequences\\_of\\_Depleted\\_Uranium\\_Use\\_in\\_the\\_U\\_S\\_Army\\_Technical\\_Report](https://www.academia.edu/25782366/Health_and_Environmental_Consequences_of_Depleted_Uranium_Use_in_the_U_S_Army_Technical_Report) Retrieved on: May 18, 2023
- M. A. McDiarmid et al., "Health effects of depleted uranium on exposed Gulf War veterans: a 10-year follow-up," *J. Toxicol. Environ. Health Part A*, vol. 67, no. 4, pp. 277 – 296, Feb. 2004. DOI: 10.1080/15287390490273541 PMID: 14713562
- A. Bleise, P. R. Danesi, W. Burkart, "Properties, use and health effects of depleted uranium (DU): a general overview," *J. Environ. Radioact.*, vol. 64, no. 2-3, pp. 93 – 112, 2003. DOI: 10.1016/s0265-931x(02)00041-3 PMID: 12500797
- Z. Hon, J. Österreicher, L. Navrátil, "Depleted uranium and its effects on humans," *Sustainability*, vol. 7, no. 4, pp. 4063 – 4077, Apr. 2015. DOI: 10.3390/su7044063

11. R. R. Parrish et al., "Depleted uranium contamination by inhalation exposure and its detection after ~ 20 years: Implications for human health assessment," *Sci. Total Environ.*, vol. 390, no. 1, pp. 58 – 68, Feb. 2008.  
DOI: 10.1016/j.scitotenv.2007.09.044  
PMid: 17976690
12. L. W. Lockett, "Radiological conditions in areas of Kuwait with residues of depleted uranium," *Health Phys.*, vol. 90, no. 2, pp. 180 – 181, Feb. 2006.  
DOI: 10.1097/00004032-200602000-00011
13. A. F. Elsayed, M. T. Hussein, S. A. El-Mongy, H. F. Ibrahim, A. Shazly, "Different Approaches to Purify the 185.7 keV of  $^{235}\text{U}$  from Contribution of Another Overlapping  $\gamma$ -Transition," *Phys. Part. Nucl. Lett.*, vol. 18, no. 2, pp 202 – 209, Mar. 2021.  
DOI: 10.1134/S1547477121020060
14. A. Aba, A. Ismaeel, "Preparation of in-house calibration source for the use in radioactivity analysis of the environmental samples: consideration of homogeneity," *J. Radioanal. Nucl. Chem.*, vol. 295, no. 1, pp. 31 – 38, Jan. 2013.  
DOI: 10.1007/s10967-012-1893-9
15. R. L. Lozano et al., "Mesoscale behavior of  $^7\text{Be}$  and  $^{210}\text{Pb}$  in superficial air along the Gulf of Cadiz (south of Iberian Peninsula)," *Atmos. Environ.*, vol. 80, pp. 75 – 84, Dec. 2013.  
DOI: 10.1016/j.atmosenv.2013.07.050
16. Y. Y. Ebaid, S. A. El-Mongy, K. A. Allam, " $^{235}\text{U}$ - $\gamma$  emission contribution to the 186 keV energy transition of  $^{226}\text{Ra}$  in environmental samples activity calculations," *Int. Cong. Ser.*, vol. 1276, pp. 409 – 411, Feb. 2005.  
DOI: 10.1016/j.ics.2004.12.020